Extended Dynamic Mode Decomposition with Jacobian Residual Penalization for Learning Bilinear, Control-affine Koopman Models

Brian E. Jackson
Robotics Institute
Carnegie Mellon University
brianjackson@cmu.edu

Jeong Hun Lee
Robotics Institute
Carnegie Mellon University
jeonghunlee@cmu.edu

Kevin Tracy
Robotics Institute
Carnegie Mellon University
ktracy@cmu.edu

Zachary Manchester
Robotics Institute
Carnegie Mellon University
zacm@cmu.edu

1 Introduction

Controlling complex, underactuated, and highly nonlinear autonomous systems remains an active area of research in robotics, despite decades of previous work exploring effective algorithms and the development of substantial theoretical analysis. Classical approaches typically rely on local linear approximations of the nonlinear system, which are then used in any of a multitude of linear control techniques, such as PID, pole placement, Bode analysis, H-infinity, LQR, or linear MPC. These approaches only work well if the states of the system always remain close to the linearization point or reference trajectory. The region for which these linearizations remain valid can be extremely small for highly nonlinear systems. Alternatively, model-based methods for nonlinear control based on optimal control have shown great success, as long as the model is well known and an accurate estimate of the global state can be provided. These model-based techniques leverage centuries of insight into dynamical systems and have demonstrated incredible performance on extremely complicated autonomous systems TODO: add citations for some recent work. On the other hand, data-driven techniques such as reinforcement learning have received tremendous attention over the last decade and have begun to demonstrate impressive performance and robustness for complicated robotic systems in unstructured environments TODO: cite a few RL results, including Marco Hutter's recent stuff. While these approaches are attractive since they require little to no previous knowledge about the system, they often require large amounts of data and fail to generalize outside of the domain or task on which they were "trained."

In this work we propose a novel method that combines the benefits of model-based and data-driven methods, based on recent work applying Koopman Operator Theory to controlled dynamical systems TODO: cite a few Koopman papers, including the CalTech ones. By leveraging data collected from an unknown dynamical system along with derivative information from an approximate analytical model, we can efficiently learn a bilinear representation of the system dynamics that performs well when used in traditional model-based control techniques such as linear MPC. The result is nonlinear dynamical system that is expressive enough to capture the full nonlinear dynamics across a broad range of the state space, but has a well-defined structure that is very amenable to specialized optimization-based controllers. By leveraging information from an analytical model, we can dramatically reduce the number of samples required to learn a good approximation of the true nonlinear dynamics.

TODO: bullet out contributions.

6th Conference on Robot Learning (CoRL 2022), Auckland, New Zealand.

TODO: add summary of paper layout.

2 Background and Related Work

2.1 The Koopman Operator

The theoretical underpinnings of the Koopman operator and its application to dynamical systems has been extensively studied, especially within the last decade TODO: cite some important theoretical works on Koopman theory here. Rather than describe the theory in detail, we highlight the key concepts employed by the current work, and defer the motivated reader to the existing literature on Koopman theory.

We start by assuming we have some discrete approximation a of controlled nonlinear, time-dynamical system whose underlying continuous dynamics are Lipschitz continuous:

$$x_{k+1} = f(x_k, u_k) \tag{1}$$

where $x \in \mathcal{X} \subseteq \mathbb{R}^{N_x}$ is the state vector and $u_k \in \mathbb{R}^{N_u}$ is the control vector. This discrete approximation can be obtained for any continuous dynamical system in many ways, including implicit and explicit Runge-Kutta methods, or by solving the Discrete Euler-Lagrange equations TODO: add citations.

The key idea behind the Koopman operator is that the nonlinear finite-dimensional discrete dynamics (1) can be represented by an infinite-dimensional *bilinear* system:

$$y_{k+1} = Ay_k + Bu_k + \sum_{i=1}^{m} u_{k,i} C_i y_k = g(y, u) \tag{2}$$

where $y = \phi(x)$ is a mapping from the finite-dimensional state space $\mathcal{X}$ to the (possibly) infinite-dimensional Hilbert space of *observables* $y \in \mathcal{Y}$. We also assume the inverse map is approximately linear: $x = Gy$. In practice, we approximate (1) by choosing ϕ to be some arbitrary finite set of nonlinear functions of the state variables, which in general include the states themselves such that the linear mapping $G \in \mathbb{R}^{N_x \times N_y}$ is exact. Intuitively, ϕ "lifts" our states into a higher dimensional space where the dynamics are approximately (bi)linear, effectively trading dimensionality for (bi)linearity. This idea should be both unsurprising and familiar to most roboticsts, since similar techniques have already been employed in other forms, such as maximal-coordinate representations of rigid body dynamics TODO: add citations, the "kernel trick" for state-vector machines TODO: add citation, or the observation that solving large, sparse nonlinear optimization problems is often more effective than solving small, tightly-coupled dense problems TODO: add citations from the trajectory optimization literature.

The lifted bilinear system (2) can be easily learned from samples of the system dynamics (x_i^+, x_i, u_i) (where x^+ is the state at the next time step) using extended Dynamic Mode Decomposition (eDMD), which is just the application of linear least squares (LLS) to the lifted states. Details of this method will be covered later when we introduce our adaptation of eDMD and present an effective numerical technique for solving the resulting LLS problems.

3 EDMD with Jacobian Residual-Penalization

Existing Koopman-based approaches to learning dynamical systems only rely on samples of the unknown dynamics. Here we present a novel method for incorporating prior knowledge about the dynamics by adding derivative information of an approximate model into the data set to be learned via eDMD.

Given P samples of the dynamics (x_i^+, x_i, u_i), and an approximate discrete dynamics model

$$x^+ = \tilde{f}(x, u) \tag{3}$$

we can evaluate the Jacobians of our approximate model $\hat{f}$ at each of the sample points: $\tilde{A}_i = \frac{\partial \tilde{f}}{\partial x}, \tilde{B}_i = \frac{\partial \tilde{f}}{\partial x}$. After choosing nonlinear mapping $\phi : \mathbb{R}^{N_x} \mapsto \mathbb{R}^{N_y}$ We then want to find a bilinear dynamics model (2) that matches the Jacobians of our approximate model, while also matching our dynamics samples. If we define $\hat{A}_j \in \mathbb{R}^{N_x \times N_x}$ and $\hat{B}_j \in \mathbb{R}^{N_x \times N_u}$ to be the Jacobians of our bilinear dynamics model, projected back into the original state space, our objective is to find the matrices $A \in \mathbb{R}^{N_y \times N_y}, B \in \mathbb{R}^{N_y \times N_u}$, and $C_{1:m} \in \mathbb{R}^{N_u} \times \mathbb{R}^{N_y \times N_y}$ that minimize the following objective:

$$(1-\alpha)\sum_{j=1}^{P} \left\|\hat{y}_j - y_j^+\right\|_2^2 + \alpha \sum_{j=1}^{P} \left\|\hat{A}_j - \tilde{A}_j\right\|_2^2 + \left\|\hat{B}_j - \tilde{B}_j\right\|_2^2 \tag{4}$$

where $\hat{y}_j^+ = g\left(\phi(x_j), u_j\right)$ is the output of our bilinear dynamics model, and $y_j^+ = \phi(y_j^+)$ is the actual lifted state (i.e. observables) at the next time step.

While not immediately apparent, we can minimize (4) using linear least-squares, using techniques similar to those used previously in the literature TODO: cite CalTech papers.

To start, we combine all the data we're trying to learn in a single matrix:

$$E = \begin{bmatrix} A & B & C_1 & \dots & C_m \end{bmatrix} \in \mathbb{R}^{N_y \times N_z} \tag{5}$$

where $N_z = N_y + N_u + N_y \cdot N_u$. We now rewrite the terms in (4) in terms of E. By defining the vector

$$z = \begin{bmatrix} y^T & u^T & u_1 y^T & \dots & u_m y^T \end{bmatrix} \in \mathbb{R}^{N_z} \tag{6}$$

we can write down the output of our bilinear dynamics (2) as

$$\hat{y}^+ = Ez. \tag{7}$$

The projected Jacobians of our bilinear model, $\hat{A}$ and $\hat{B}$, are simply the Jacobians of the bilinear dynamics in terms of the original state. We obtain these dynamics by "lifting" the state via ϕ and then projecting back onto the original states using G:

$$x^+ = G\left(A\phi(x) + Bu + \sum_{i=1}^{m} u_i C_i \phi(x)\right) = \hat{f}(x,u) \tag{8}$$

Differentiating these dynamics give us our projected Jacobians:

$$\hat{A}_j = G\frac{\partial \hat{f}}{\partial x}(x_j, u_j) = G\left(A + \sum_{i=1}^{m} u_{j,i} C_i\right)\Phi(x_j) = GE\bar{A}(x_j, u_j) = GE\bar{A}_j \tag{9a}$$

$$\hat{B}_i = G\frac{\partial \hat{f}}{\partial u}(x_j, u_j) = G\Big(B + \begin{bmatrix} C_1 x_j & \dots & C_m x_j \end{bmatrix}\Big) = GE\bar{B}(x_j, u_j) = GE\bar{B}_j \tag{9b}$$

where $\Phi(x) = \partial\phi/\partial x$ is the Jacobian of the nonlinear map ϕ, and

$$\bar{A}(x,u) = \begin{bmatrix} I \\ 0 \\ u_1 I \\ u_2 I \\ \vdots \\ u_m I \end{bmatrix} \in \mathbb{R}^{N_z \times N_x}, \quad \bar{B}(x,u) = \begin{bmatrix} 0 \\ I \\ [x\ 0\ \dots\ 0] \\ [0\ x\ \dots\ 0] \\ \vdots \\ [0\ 0\ \dots\ x] \end{bmatrix} \in \mathbb{R}^{N_z \times N_u}. \tag{10}$$

Substituting (7) and (9) into (4), we can rewrite our LLS problem as:

$$\underset{E}{\text{minimize}} \quad \sum_{j=0}^{P} (1-\alpha)\left\|Ez_j - y_j^+\right\|_2^2 + \alpha\left\|GE\bar{A}_j - \tilde{A}_j\right\|_2^2 + \alpha\left\|GE\bar{B}_j - \tilde{B}_j\right\|_2^2 \tag{11}$$

which is equivalent to

$$\underset{E}{\text{minimize}} \quad (1-\alpha)\left\|E\mathbf{Z_{1:P}} - \mathbf{Y_{1:P}^+}\right\|_2^2 + \alpha\left\|GE\bar{\mathbf{A}}_{\mathbf{1:P}} - \tilde{\mathbf{A}}_{\mathbf{1:P}}\right\|_2^2 + \alpha\left\|GE\bar{\mathbf{B}}_{\mathbf{1:P}} - \tilde{\mathbf{B}}_{\mathbf{1:P}}\right\|_2^2 \tag{12}$$

where $\mathbf{Z_{1:P}} \in \mathbb{R}^{N_z \times P} = [z_1 \ z_2 \ ... \ z_P]$ horizontally concatenates all of the samples (equivalent definition for $\mathbf{Y^+_{1:P}} \in \mathbb{R}^{N_y \times P}$, $\bar{\mathbf{A}}_{\mathbf{1:P}} \in \mathbb{R}^{N_z \times N_x \cdot P}$, $\tilde{\mathbf{A}}_{\mathbf{1:P}} \in \mathbb{R}^{N_z \times N_x \cdot P}$, $\bar{\mathbf{B}}_{\mathbf{1:P}} \in \mathbb{R}^{N_z \times N_u \cdot P}$, and $\tilde{\mathbf{B}}_{\mathbf{1:P}} \in \mathbb{R}^{N_z \times N_u \cdot P}$).

We can rewrite (14) in standard form using the "vec trick"

$$\text{vec}(AXB) = (B^T \otimes A)\text{vec}(X) \tag{13}$$

where $\text{vec}(A)$ stacks the columns of A into a single vector.

Setting E in (14) equal to X in (13), we get

$$\underset{E}{\text{minimize}} \left\| \begin{bmatrix} (1-\alpha) \cdot (\mathbf{Z_{1:P}})^T \otimes I_{N_y} \\ \alpha \cdot (\bar{\mathbf{A}}_{\mathbf{1:P}})^T \otimes G \\ \alpha \cdot (\bar{\mathbf{G}}_{\mathbf{1:P}})^T \otimes G \end{bmatrix} \text{vec}(E) + \begin{bmatrix} (1-\alpha) \cdot \text{vec}(\mathbf{Y^+_{1:P}}) \\ \alpha \cdot \text{vec}(\tilde{\mathbf{A}}_{\mathbf{1:P}}) \\ \alpha \cdot \text{vec}(\tilde{\mathbf{G}}_{\mathbf{1:P}}) \end{bmatrix} \right\|_2^2 \tag{14}$$

such that the matrix of cofficients has $(N_y + N_x^2 + N_x \cdot N_u) \cdot P$ rows and $N_y \cdot N_z$ columns.

4 Results

All continuous dynamics were discretized with an explicit fourth-order Runge Kutta integrator.

4.1 Training

All models were trained by simulating the "real" system with an arbitrary controller to collect data in the region of the state space relevant to the task. A set of fixed-length trajectories were collected, each at a sample rate of 20 Hz. The bilinear eDMD model was trained using the same approach in [1]. For the proposed jDMD method, the Jacobians of the nominal model were calculated at each of the sample points and the bilinear model was learned using the approach outlined in Section 3.

4.2 Cartpole

As a simple benchmark example, we use the canonical cartpole system. In lieu of an actual hardware experiment (left for future work), we specify two separate analytical models used in simulation: the *nominal* model is a simple cartpole system without friction or damping, whereas the *simulated* model, used exclusively for simulating the system in place of a real hardware platform, includes viscous damping on both degrees of freedom, a tanh Coloumb friction model for the cart, and a deadband on the control signal. Additionally, we altered the mass of the cart and pole from the nominal model by 20% and 25%, respectively. See the provided code for the actual values and models used in the experiments.

We split the analysis of this system into two separate tasks: stabilization about the upward unstable equilibrium from perturbed initial condtions, and the swing-up task where the system must successfully stabilize after starting from the downward equilibrium.

4.2.1 Stabilization

For stabilizing the system about the upward unstable equilibrium 50 initial conditions were collected using an LQR controller designed using the nominal model. The a basis function of $\phi(x) = [\ 1,\ x,\ \sin(x),\ \cos(x),\ \sin(2x)\ ] \in \mathbb{R}^{17}$ was used. After learning both models, LQR and MPC controllers were designed using the nominal, eDMD, and jDMD model. For the learned bilinear models, a controller was designed using both the Jacobians of the bilinear dynamics and the projected Jacobians (9). The MPC controllers linearized the dynamics about the equilibrium and solved the resulting equality-constrained quadratic program using Riccati recursion and a horizon of 41 time steps (2 seconds). Each controller was tested using 100 different initial conditions. The distance of the state after 4 seconds for the LQR and MPC controllers is shown in Figure

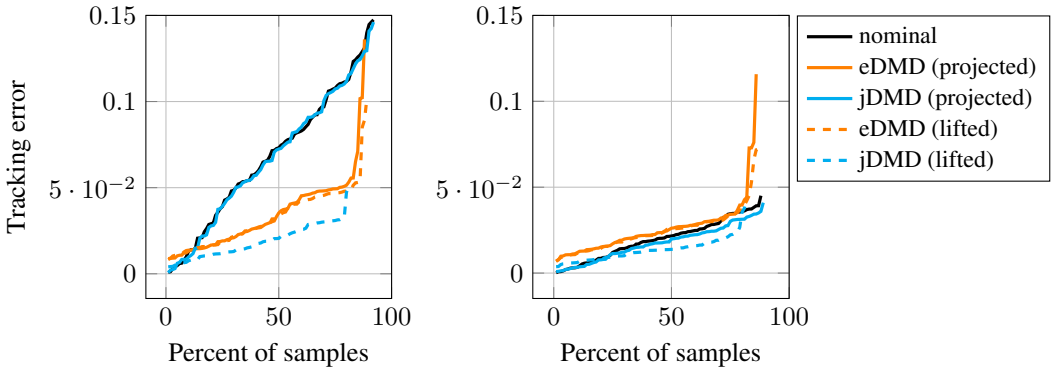

(a) LQR Controllers

(b) MPC Controller

Figure 1: Controller performance on the task of stabilizing the cartpole system about the upward unstable equilibrium. Performance is plotted as the error

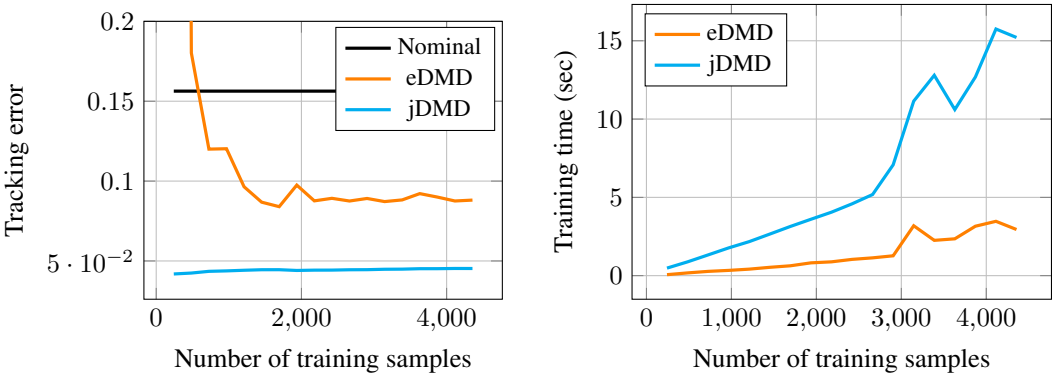

(a) MPC tracking error vs training samples for the cartpole. Tracking error is defined as the average L2 error over all the test trajectories between the reference and simulated trajectories. The proposed jDMD method immediately learns a model good enough for control with just a couple hundred dynamics samples (2 swing-up trajectories).

(b) Training time for cartpole models as a function of training samples. The training time complexity is approximately linear.

4.2.2 MPC Tracking Performance

To train the bilinear model for the swing-up task, we generated 50 training swing-up trajectories using ALTRO, an open-source nonlinear trajectory optimization solver [2, 3], on the nominal cartpole model. Each trajectory was 5 seconds long and sampled at 20 Hz. A linear MPC controller was then used to track the swing-up trajectories on the simulated system, resulting in significant tracking error due to the model mismatch. After learning both models, a linear MPC policy was used to track the original swing-up trajectory generated by ALTRO. The MPC policy linearized the dynamics about the reference trajectory, used a quadratic penalty on deviations from the reference, and was solved using Riccati recursion for a horizon of 41 time steps (2 seconds). To successfully stabilize the system at the upward equilibrium, the MPC policy extrapolated the terminal state and control reference indefinitely. For each of the bilinear models, the Jacobians were projected back onto space of the original dynamics, resulting in an MPC policy that was just as efficient to solve online as the nominal model (all controllers ran at several thousand Hertz without much performance tuning).

The tracking error, defined as the average L2 norm of the error between the reference trajectory and the actual trajectory of the simulated system for 10 test trajectories not included in the training

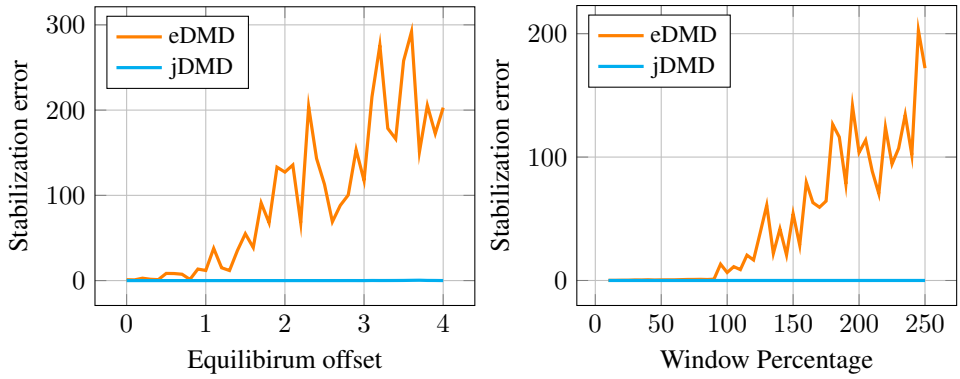

(a) LQR stabilization with equilibrium offset

(b) LQR stabilization with varying "window" of initial condition sampling

Figure 3: LQR controller robustness to varying initial conditions and equilibrium offset

data, was recorded after training both the eDMD and jDMD models with an increasing number of trajectories. The results in Figure 6a clearly show that jDMD produces a high-quality model with extremely few samples, whereas eDMD—even after many training samples—never achieves the same level of performance. The lack of progress with increasing samples is likely a result of poor variety in the training data: after enough samples both methods effectively learn all the information that can be learned from the distribution from which the training data is sampled. This example highlights the value of adding even just a little derivative information to a data-driven approach: it dramatically increases sample efficiency while also improving the quality of the learned model, especially when that model is used in optimization-based controllers such as MPC that rely on derivative information. For reference, the training times are shown in Figure 6b. Note that the training algorithms haven't yet been optimized for max performance but reflect a decent first implementation.

4.3 Planar Quadrotor

As another benchmark example, we use the planar quadrotor model, a simplification of the full quadrotor system with only 3 degrees of freedom. Like the cartpole study, we once again specify two separate analytical models used in simulation: the *nominal* model is a simple planar quadrotor system without aerodynamic drag, whereas the *simulated* model, used exclusively for simulating the system in place of a real hardware platform, includes aerodynamic drag, which acts as a viscous damping force. Additionally, we altered the system properties (e.g. mass, rotor arm length, etc.) by 5% to incorporate additional mismatch between the nominal and simulated model. See the provided code for the actual values and models used in the experiments.

4.3.1 Stabilization

For stabilizing the system about the upward unstable equilibrium 50 initial conditions were collected using an LQR controller designed using the nominal model. The a basis function of $\phi(x) = [\ 1,\ x,\ \sin(x),\ \cos(x),\ \sin(2x)\ ] \in \mathbb{R}^{17}$ was used. After learning both models, LQR and MPC controllers were designed using the nominal, eDMD, and jDMD model. For the learned bilinear models, a controller was designed using both the Jacobians of the bilinear dynamics and the projected Jacobians (9). The MPC controllers linearized the dynamics about the equilibrium and solved the resulting equality-constrained quadratic program using Riccati recursion and a horizon of 41 time steps (2 seconds). Each controller was tested using 100 different initial conditions. The distance of the state after 4 seconds for the LQR and MPC controllers is shown in Figure

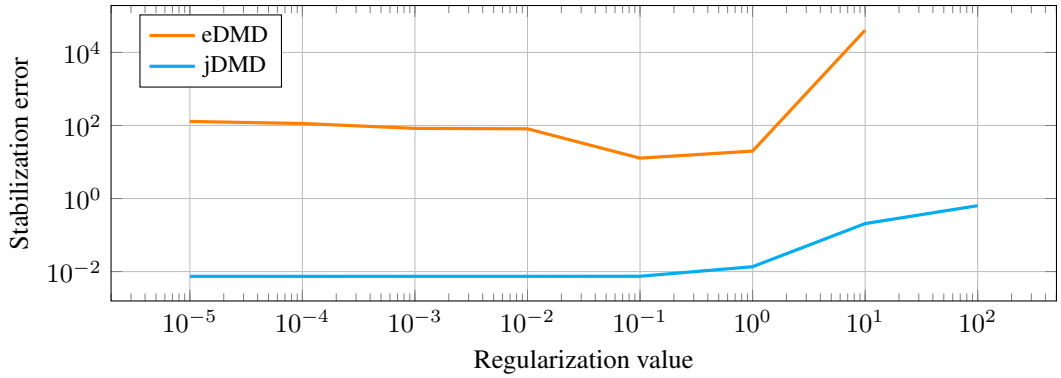

Figure 4: LQR stabilization with equilibrium offset

Figure 5: Robustness of jDMD and eDMD to regularization value. jDMD much more robust

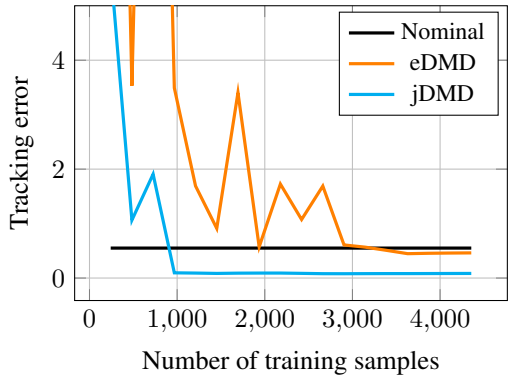

(a) MPC tracking error vs training samples for the cartpole. Tracking error is defined as the average L2 error over all the test trajectories between the reference and simulated trajectories. The proposed jDMD method immediately learns a model good enough for control with just a couple hundred dynamics samples (2 swing-up trajectories).

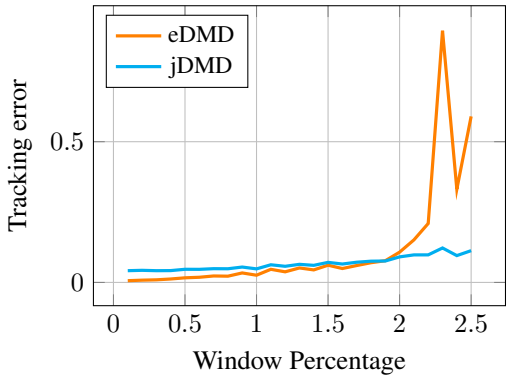

(b) MPC tracking error of quadrotor for various ranges of which to sample initial conditions. Percentage is determined by the limits of the range of training data, where 100% is the limit of the training data's range

4.3.2 MPC Tracking Performance

References

[1] C. Folkestad and J. W. Burdick. Koopman NMPC: Koopman-based Learning and Nonlinear Model Predictive Control of Control-affine Systems. pages 7350–7356, oct 2021. ISSN 10504729. doi:10.1109/ICRA48506.2021.9562002.

[2] T. A. Howell, B. E. Jackson, and Z. Manchester. ALTRO: A Fast Solver for Constrained Trajectory Optimization. *IEEE International Conference on Intelligent Robots and Systems*, pages 7674–7679, nov 2019. ISSN 21530866. doi:10.1109/IROS40897.2019.8967788.

[3] B. E. Jackson, T. Punnoose, D. Neamati, K. Tracy, R. Jitosho, and Z. Manchester. ALTRO-C: A Fast Solver for Conic Model-Predictive Control; ALTRO-C: A Fast Solver for Conic Model-Predictive Control. *2021 IEEE International Conference on Robotics and Automation (ICRA)*, 2021. doi:10.1109/ICRA48506.2021.9561438. URL `https://github.com/`.